LETTER

doi:10.1038/nature22795

Human fetal dendritic cells promote prenatal T-cell immune suppression through arginase-2

Naomi McGovern[1], Amanda Shin[1,2], Gillian Low[1], Donovan Low[1], Kaibo Duan[1], Leong Jing Yao[3], Rasha Msallam[1], Ivy Low[1], Nurhidaya Binte Shadan[1], Hermi R Sumatoh[1], Erin Soon[1], Josephine Lum[1], Esther Mok[1], Sandra Hubert[1], Peter See[1], Edwin Huang Kunxiang[4], Yie Hou Lee[5,6], Baptiste Janela[1], Mahesh Choolani[7,8], Citra Nurfarah Zaini Mattar[7,8], Yiping Fan[4,8], Tony Kiat Hon Lim[9], Dedrick Kok Hong[9], Ker-Kan Tan[10,11], John Kit Chung Tam[11], Christopher Schuster[12], Adelheid Elbe-Bürger[12], Xiao-nong Wang[13], Venetia Bigley[13], Matthew Collin[13], Muzlifah Haniffa[13], Andreas Schlitzer[1,14,15], Michael Poidinger[1], Salvatore Albani[3], Anis Larbi[1], Evan W Newell[1], Jerry Kok Yen Chan[1,4,8,16]* & Florent Ginhoux[1]*

During gestation the developing human fetus is exposed to a diverse range of potentially immune-stimulatory molecules including semi-allogeneic antigens from maternal cells[1,2], substances from ingested amniotic fluid[3,4], food antigens[5], and microbes[6]. Yet the capacity of the fetal immune system, including antigen-presenting cells, to detect and respond to such stimuli remains unclear. In particular, dendritic cells, which are crucial for effective immunity and tolerance, remain poorly characterized in the developing fetus. Here we show that subsets of antigen-presenting cells can be identified in fetal tissues and are related to adult populations of antigen-presenting cells. Similar to adult dendritic cells, fetal dendritic cells migrate to lymph nodes and respond to toll-like receptor ligation; however, they differ markedly in their response to allogeneic antigens, strongly promoting regulatory T-cell induction and inhibiting T-cell tumour-necrosis factor-α production through arginase-2 activity. Our results reveal a previously unappreciated role of dendritic cells within the developing fetus and indicate that they mediate homeostatic immune-suppressive responses during gestation.

We used a combination of flow cytometry and gene array analysis to characterize human fetal antigen-presenting cells (APC) and compare them with adult APC. Using our previously described gating strategy for adult tissue APC[7,8] (Extended Data Fig. 1a, b), we identified fetal APC subsets: $CD14^+$ monocytes/macrophages, plasmacytoid dendritic cells (pDC), conventional (c)DC1, and cDC2 within fetal spleen, skin (in agreement with findings by others[9]), thymus, and lung (Fig. 1a and Extended Data Fig. 1a) by 13 weeks estimated gestational age (EGA). Within both early (12–15 weeks) and late (16–22 weeks) second-trimester fetal tissue, APC were relatively abundant within the $CD45^+$ compartment compared with adult tissues (Fig. 1b and Extended Data Fig. 1c). Fetal spleen cDC1 and cDC2 were also observed *in situ* using immunofluorescence microscopy (Extended Data Fig. 1d). Next we compared the gene expression profiles of cDC1, cDC2, and $CD14^+$ cells from fetal skin and spleen with those from adult spleen (for sort gating strategy, see Extended Data Fig. 1a, b; for post-sort cell purity confirmation, see Extended Data Fig. 2a) as well as with published data on adult blood- and skin-derived APC subsets (Supplementary Experimental Procedures, Extended Data Fig. 3 and ref. 7). Connectivity map analysis[7] was used to compare the subset-specific gene expression signatures of fetal spleen and skin cDC1, cDC2, and $CD14^+$ cells with those of adult blood, skin, and spleen APC (Fig. 1c). Connectivity map scores indicated that the gene expression signature of fetal cDC1 was enriched with genes also expressed by adult cDC1; similarly, the fetal cDC2 signature was enriched with adult cDC2-associated genes and fetal $CD14^+$ cells scored most highly with adult blood monocyte and tissue macrophage populations, as expected[7,8]. Scatter plot analysis of normalized gene expression confirmed the strong correlation ($R = 0.92$) between the expression profiles of fetal and adult cDC1, as well as fetal and adult cDC2 (Extended Data Fig. 2b). Conserved gene lists across fetal and adult APC subsets and ingenuity pathway analysis of these gene lists are provided in Supplementary Tables 1–9 (see Supplementary Experimental Procedures for the analysis). At the molecular level, fetal and adult dendritic cells expressed comparable levels of dendritic cell subset-specific transcription factors (Extended Data Fig. 2c), in agreement with published data[10]. Detailed phenotyping by CyTOF and One-SENSE analysis (see Supplementary Experimental Procedures and ref. 11) demonstrated that fetal and adult spleen dendritic cells had similar antigen expression profiles, except for CD141, FcεR1, and CLA, which were relatively more highly expressed on adult cDC2 (Extended Data Fig. 4a, b).

To gain insight into the functions and heterogeneity of the fetal tissue cDC populations, we first compared their surface antigen expression profiles across tissues within single donors (Fig. 2a; input gating strategy and original heatmap in Extended Data Fig. 5a, b), and with cDC from adult tissues using CyTOF and One-SENSE analysis[11] (Extended Data Fig. 5c). Fetal cDC1 and cDC2 showed great heterogeneity between tissues at the single-cell level (Fig. 2a), most obviously within the lung, suggesting differential tissue imprinting. We also identified tissue-specific cDC phenotypes conserved between adults and fetuses (Extended Data Fig. 5c). For example, both fetal and adult lung cDC2 expressed elevated levels of CD2 and FcεR1, while expression of these markers by fetal and adult gut cDC were low to negative. Notably, the fetal lung cDC2 population exhibited heterogeneous expression of the transcription factor interferon-regulatory factor (IRF)-4 (Extended

[1]Singapore Immunology Network (SIgN), A*STAR, 8A Biomedical Grove, Immunos Building, Level 3 and 4, Singapore 138648, Singapore. [2]Shanghai Institute of Immunology, Shanghai Jiao Tong University School of Medicine, Shanghai, 200025, China. [3]Singhealth Translational Immunology and Inflammation Centre (STIIC), 20 College Road, the Academia, Level 8 Discovery Tower, Singapore 169856, Singapore. [4]Department of Reproductive Medicine, KK Women's and Children's Hospital, Singapore 229899, Singapore. [5]KK Research Centre, KK Women's and Children's Hospital, 100 Bukit Timah Road, Singapore 229899, Singapore. [6]OBGYN-Academic Clinical Program, Duke-NUS, Duke-NUS Medical School, 8 College Road, Singapore 169857, Singapore. [7]Department of Obstetrics & Gynaecology, Yong Loo Lin School of Medicine, National University of Singapore, NUHS Tower Block, 1E Kent Ridge Road, Singapore 119228, Singapore. [8]Experimental Fetal Medicine Group, Yong Loo Lin School of Medicine, National University of Singapore, Singapore 119077, Singapore. [9]Department of Pathology, Singapore General Hospital, 20 College Road, Singapore 169856, Singapore. [10]Division of Colorectal Surgery, University Surgical Cluster, National University Health System, Singapore 119074, Singapore. [11]Department of Surgery, Yong Loo Lin School of Medicine, National University of Singapore, 1E Kent Ridge Road, Singapore 119228, Singapore. [12]Department of Dermatology, DIAID, Medical University of Vienna, Währinger Gürtel 18-20, 1090 Vienna, Austria. [13]Institute of Cellular Medicine, Newcastle University, Newcastle upon Tyne NE2 4HH, UK. [14]Myeloid Cell Biology, Life and Medical Science Institute, University of Bonn, 53115 Bonn, Germany. [15]Single Cell Genomics and Epigenomics Unit at the German Center for Neurodegenerative Diseases and the University of Bonn, 53175 Bonn, Germany. [16]Cancer and Stem Cell Biology Program, Duke-NUS Graduate Medical School, Singapore 119077, Singapore.
*These authors contributed equally to this work.

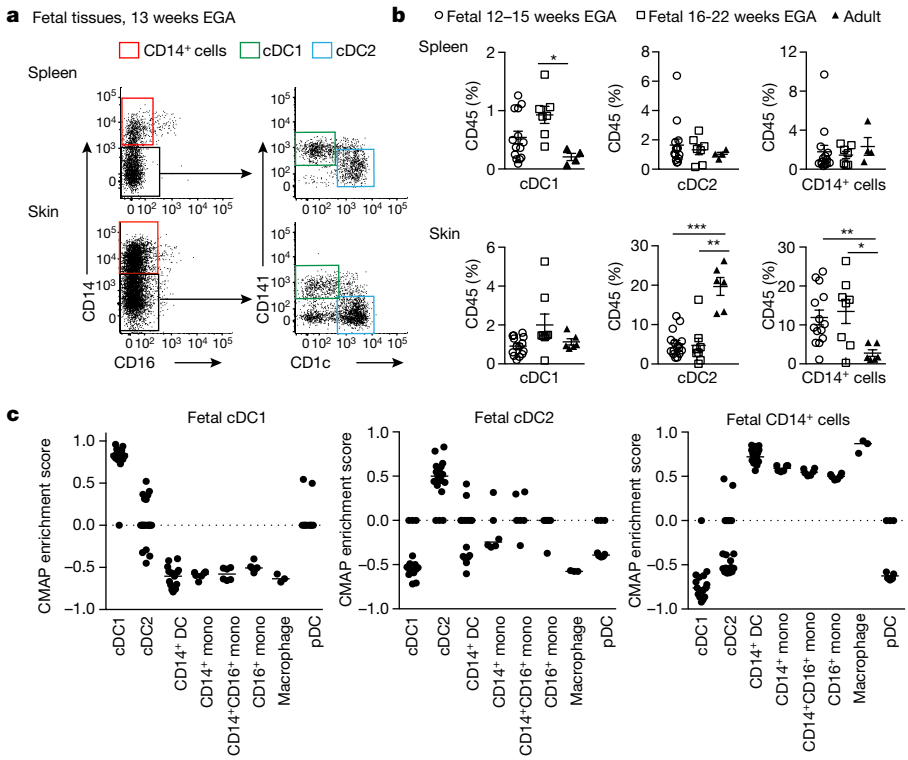

Figure 1 | Identification of fetal APC. a, $CD14^+$, cDC1, and cDC2 cells were identified within fetal spleen and skin by flow cytometry. **b**, Enumeration of APC subsets within fetal and adult tissues. Mann–Whitney test $*P<0.05$, $**P<0.01$, $***P<0.001$. Mean ± s.e.m. **c**, Connectivity map (CMAP) enrichment scores for fetal skin and spleen cDC1, cDC2, and $CD14^+$ cells against all adult blood, skin, and spleen APC subsets are shown. Enrichment scores for fetal skin and spleen cDC1, cDC2, and $CD14^+$ cells with equivalent adult APC subsets were significant at $P<0.0001$. **a**, **b**, Each data point in the scatter plots represents an individual experiment.

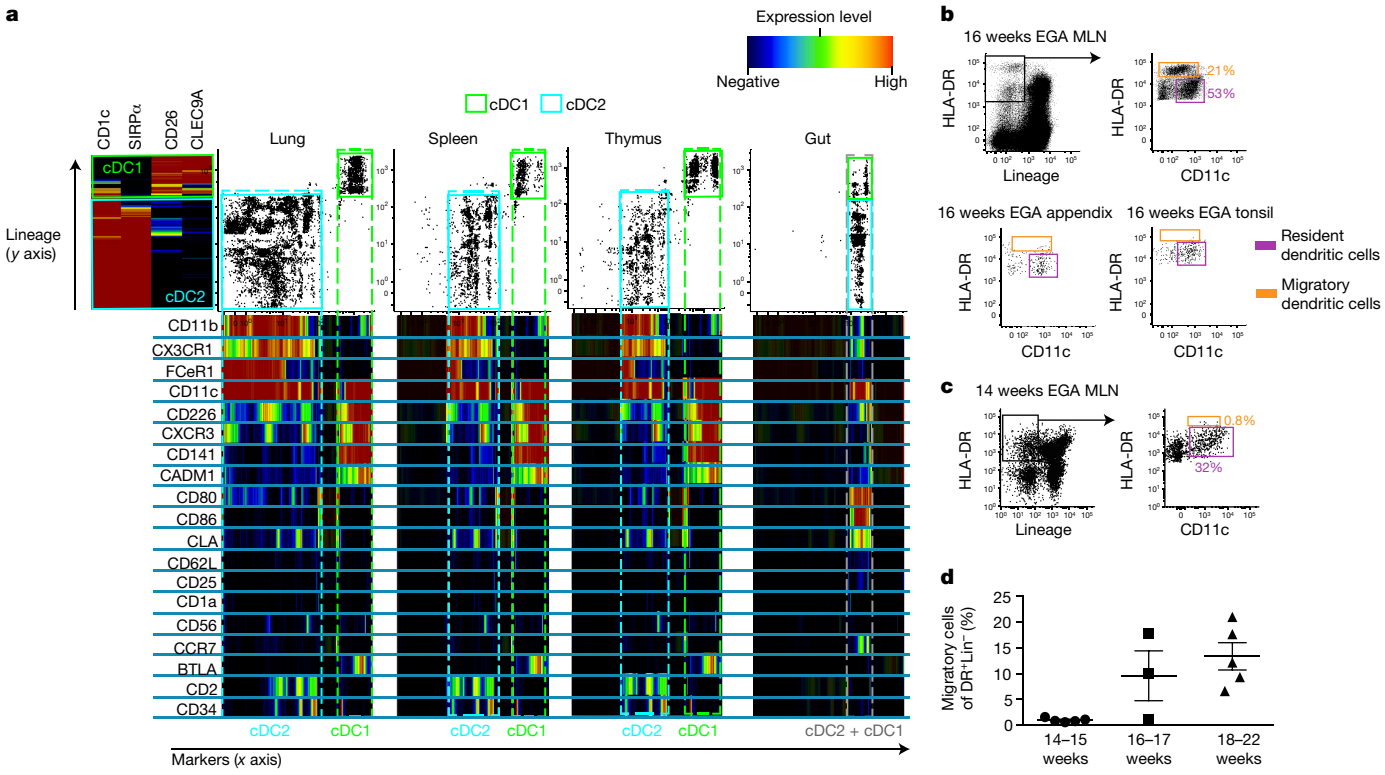

Figure 2 | Fetal cDC migrate to draining lymph nodes. a, Characterization of cDC1 and cDC2 across fetal tissues using CyTOF and One-SENSE algorithm (see Methods, representative plots of $n=5$). **b**, **c**, Flow cytometry analysis of fetal MLN at 16 weeks (**b**) or 14 weeks (**c**) EGA. Within the $HLA\text{-}DR^+Lin^-$ gate (black), $HLA\text{-}DR^{int}CD11c^{hi}$ resident dendritic cells (pink) were distinguished from $HLA\text{-}DR^{hi}CD11^{int}$ migratory dendritic cells (orange gate). **b**, Sixteen week EGA MLN (left) and fetal appendix and tonsil (right, $n=3$). **d**, Enumeration of migratory cDC at indicated time points. Mean ± s.e.m. Each data point in the scatter plots represents an individual experiment.

Data Fig. 5d), which indicated contamination of the gated population with monocytes and/or monocyte-derived cells, as seen in adults[12]. Several activation markers were differentially expressed between cDC from different fetal tissues. In particular, fetal gut cDC displayed a more activated phenotype than did cDC in other fetal tissues (Fig. 2 a and Extended Data Fig. 5b, c), expressing higher levels of the chemokine receptor CCR7 and the activation markers CD80 and CD86. As CCR7 mediates dendritic cell migration to lymph nodes in adults, where they initiate and shape emergent T-cell responses[8,13], we then asked whether CCR7$^+$ gut dendritic cells migrated to their draining lymphoid organs during fetal life. Using a gating strategy verified in adult tissues[7], we identified migratory (HLA-DR^{hi}CD11c$^{lo/int}$) and resident (HLA-DR^{int}CD11c^{hi}) dendritic cells in 16 week EGA fetal mesenteric lymph nodes (MLN) (Fig. 2b). In contrast, in the fetal appendix and tonsil, which lack connecting afferent lymphatics, we observed only resident dendritic cells (Fig. 2b). Within the MLN, the resident cell population included CD14$^+$, cDC1 (CD26$^+$CD1c$^-$), and cDC2 (CD26$^-$CD1c$^+$) cells (Extended Data Fig. 6a). The migratory-phenotype fraction of dendritic cells within the MLN contained relatively few CD14$^+$ cells, as in adults[7,8], alongside both cDC1 and cDC2, with the former relatively more abundant (Extended Data Fig. 6a, b). Of note, fetal gut cDC1 expressed more CCR7 than did cDC2 (Extended Data Fig. 5c). Similar to adult migratory dendritic cells[7], fetal MLN migratory dendritic cells expressed higher levels of CCR7 and the activation markers CD80, CD83, and CD86 than did dendritic cells with the resident phenotype (Extended Data Fig. 6c). Looking along the timeline of the second trimester of gestation, we found that while 14–15 week EGA MLN contained abundant resident dendritic cells, migratory dendritic cells were scarce or absent (Fig. 2c, d), suggesting that fetal gut dendritic cells begin migrating to the MLN from 16 to 17 weeks EGA. The presence of migratory dendritic cells in the MLN is consistent with expression of the lymph-node-homing cytokines CCL19 and CCL21 (ref. 14) in the fetal gut and MLN (Extended Data Fig. 6d, e). Migratory HLA-DR$^+$ cells were also visualized within the lymphatic vessels (LYVE-1$^+$) of 17–22 week EGA fetal skin (Extended Data Fig. 6f and ref. 8), providing confirmation that fetal cDC can migrate via lymphatic vessels *in vivo*. Furthermore, we observed fetal dendritic cells migrating out of skin explants over a period of 48 h (Extended Data Fig. 6g), using *ex vivo* skin assays validated in adult tissues[15]. In summary, our data suggest that fetal skin and gut dendritic cells have the capacity to migrate through lymphatics and to lymph nodes from 16 weeks EGA, where they may interact with fetal T cells that are present in lymphoid organs from 10 weeks EGA[16]. The reason for the initiation of dendritic cell migration to the lymph nodes around 16 weeks EGA remains unclear: while the human lymphatic system is in place by 8 weeks EGA, it may remain functionally immature for some time thereafter[17].

Next, we asked whether fetal cDC were able to respond toll-like receptor (TLR)[18] stimulation and/or to activate naive T cells *in vitro*. Sorted splenic cDC2 (most abundant cDC subset) from 17 to 22 week EGA fetuses and adult samples were exposed to a panel of TLR agonists: adult and fetal cells secreted similar amounts of the pro-inflammatory cytokines GM-CSF, IL-6, IL-8, and MIP-1β (Fig. 3a and Extended Data Fig. 7a), in line with their similar expression of pattern recognition receptors (Extended Data Fig. 7b). Moreover, fetal and adult splenic cDC2 induced comparable proliferation of allogeneic carboxyfluorescein succinimidyl ester (CFSE)-labelled adult splenic T cells in a mixed lymphocyte reaction (Fig. 3b). Thus fetal cDC are capable of both sensing pathogens and stimulating T cells, which, together with their migratory ability, indicates that they have the potential to initiate an immune response to microbe-derived products around 17 weeks EGA.

While this shows that fetal cDC are capable of initiating allogeneic T-cell proliferation *in vitro*, we know that lifelong *in vivo* tolerance towards non-inherited maternal allogeneic antigens is established during gestation[2,9,19]. Thus, to understand how fetal dendritic cells contribute to such tolerogenic T-cell responses, we examined the phenotype of the T-cell populations generated from mixed lymphocyte

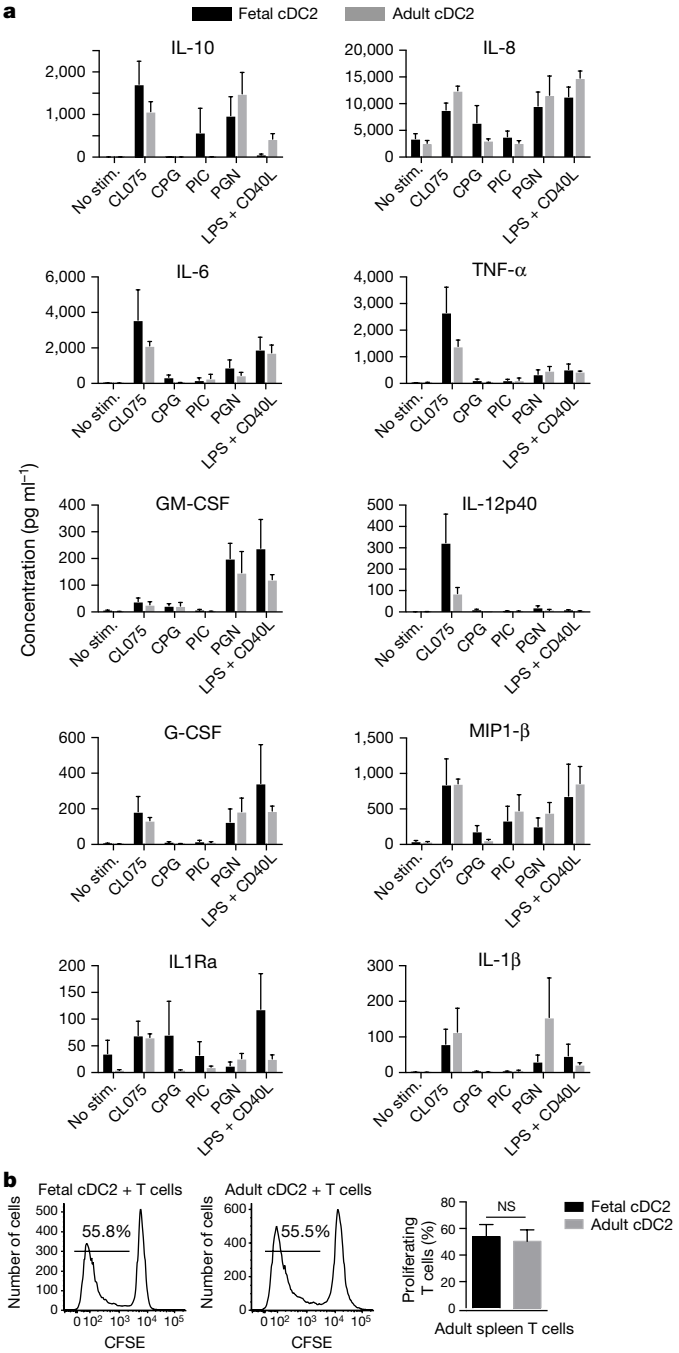

Figure 3 | Fetal cDC are responsive to TLR stimulation and induce T-cell proliferation. a, Cytokines in supernatants of fetal and adult cDC2 stimulated for 18 h with TLR agonists: CL075 (1 μg ml^{-1}), CpG oligodeoxynucleotides (CpG) (3 μM), polyinosinic-polycytidylic acid (PI:C) (25 μg ml^{-1}), peptidoglycan (PGN) (10 μg ml^{-1}), lipopolysaccharide (LPS) (0.1 μg ml^{-1}) + CD40 ligand (CD40L) (1 μg ml^{-1}). No stim., no stimulation. Mean ± s.e.m., $n = 4$. **b**, Alloactivation of adult CD4$^+$ T cells by fetal and adult cDC2 after co-culture for 6 days. Proliferation was measured by CFSE dilution. Left: representative histograms. Right: cumulative data, $n = 5$. Mean ± s.e.m. NS, not significant ($P > 0.05$), Mann–Whitney test.

reaction, where fetal or adult cDC2 were co-cultured with allogeneic adult spleen T cells. After co-culture for 6 days, fetal spleen cDC2 induced the differentiation of significantly higher frequencies of CD4$^+$CD25$^+$FOXP3$^+$CD127$^-$CTLA4$^+$ bona fide T regulatory cells (T_{reg})[1,20,21] than did adult splenic cDC2 (Extended Data Fig. 8a–c). Confirming the immunosuppressive capacity of fetal cDC2-induced

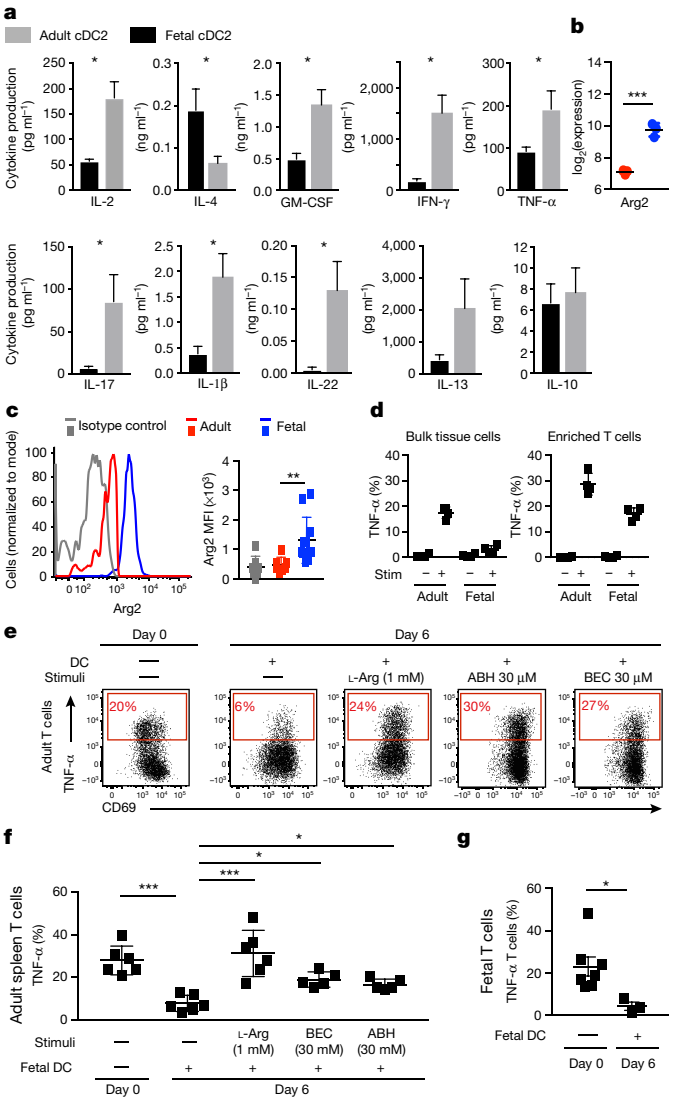

Figure 4 | Arginase-2$^+$ fetal cDC regulate TNF-α production. **a**, Cytokine production by adult T cells after co-culture for 6 days with fetal or adult cDC2 ($n = 5$). **b**, **c**, Expression of arginase-2 gene (**b**) and protein (**c**) in cDC2. **d**, Splenocyte T-cell TNF-α production. **e**, **f**, TNF-α production (red) of stimulated adult T cells, after overnight culture in the absence (day 0) or presence of cDC2 (day 6 of co-culture), with or without additional supplementation of L-arginine or arginase inhibitors (ABH or BEC). **e**, Representative dot plots. **f**, Cumulative data. **g**, TNF-α production from stimulated fetal T cells under indicated culture conditions. Mean ± s.e.m. $^*P < 0.05$, $^{**}P < 0.01$, $^{***}P < 0.001$, Mann–Whitney test. Each data point in the scatter plots represents an individual experiment.

T_{reg} cells, CD8$^+$ T-cell proliferation was significantly impaired upon co-culture with fetal cDC2 as opposed to adult cDC2 (Extended Data Fig. 8d), and was restored when CD4$^+$ T cells were removed (Extended Data Fig. 8e). In addition, allogeneic T cells cultured with fetal cDC2 (Fig. 4a) or cDC1 (Extended Data Fig. 8f) produced significantly less of several pro-inflammatory cytokines and significantly more of the Th2-polarizing cytokine IL-4, but not IL-13, compared with allogeneic T cells incubated with adult cDC2. Thus, consistent with the establishment of fetal tolerance to maternal antigens *in vivo*, fetal cDC initiate T_{reg} induction and do not launch T-cell pro-inflammatory responses *in vitro*.

The observed functional differences between fetal and adult dendritic cells were mirrored at their gene expression level, with over 3,000 genes being significantly differentially expressed between fetal and adult APC (Extended Data Fig. 9a and Supplementary Tables 10 and 11). Ingenuity pathway analysis revealed that multiple pathways involved in educating T cells were significantly differentially regulated between fetal and adult APC, as were several pathways involved in the inducible nitric oxide synthase/tumour-necrosis factor-α (iNOS/TNF-α) axis (Extended Data Fig. 9b, red and black arrows, respectively, Supplementary Table 12). Further analysis revealed that a number of genes involved in immune suppression/inflammation were differentially expressed (Extended Data Fig. 9c). Of particular interest was the elevated expression of arginase-2 by fetal spleen cDC2 (Fig. 4b, c) and cDC1 (Extended Data Fig. 9d, e) in comparison with adult spleen cDC. Of note, arginase-2 expression was not modulated by TLR stimulation (Extended Data Fig. 9f). Arginase depletes the local environment of L-arginine (by converting L-arginine to L-ornithine and urea) which is required for the production of TNF-α[22,23]. Importantly, arginase activity has been shown to be an essential player in the regulation of TNF-α levels in the neonate[22].

Coincidingly, we found that in stimulated splenic culture (that is, include APC), fetal T cells did not produce TNF-α compared with adult T cells (Fig. 4d and Extended Data Fig. 10a). However, when enriched (that is, in the absence of APC), they produced TNF-α, although to a lesser level to their adult counterparts (Fig. 4d). Furthermore, we found significantly lower frequencies of fetal T cells producing TNF-α than adult T cells after 6 days of culture (Extended Data Fig. 10b). In addition, when fetal and adult splenocytes were co-cultured at increasing ratios of fetal cells, adult T-cell TNF-α production was impaired. While fetal splenocytes also promoted T_{reg} induction, the change in TNF-α levels did not correlate with the change observed in T_{reg} induction (Extended Data Fig. 10b–d). These data suggested that the differential arginase-2 expression between adult and fetal cDC is sufficient to regulate T-cell responses and their TNF-α production.

In the absence of any cDC, approximately 24% of proliferating adult splenic T cells produced TNF-α, while after co-culture for 6 days with fetal cDC2 (Fig. 4e, f) or cDC1 (Extended Data Fig. 9g) expressing arginase-2, their ability to produce TNF-α was dramatically reduced. TNF-α production was reinstated upon replenishing the medium with L-arginine or by the addition of arginase-specific inhibitors[22] (Fig. 4e, f), confirming that the reduced TNF-α production was mediated through cDC arginase-2 activity. T_{reg} numbers did not change when arginase activity was modulated, suggesting that fetal dendritic cell regulation of TNF-α production is independent of their promotion of T_{reg} induction (Extended Data Fig. 10e–h). Further analysis of the supernatants from the co-cultures found that fetal cDC did not downregulate T-cell production of other pro-inflammatory cytokines by arginase-2 activity (Extended Data Fig. 10i–k), suggesting fetal dendritic cells utilize a range of mechanisms to regulate T-cell biology, which remain to be explored. We also found that when fetal cDC were cultured with adult cDC2, they could abrogate adult cDC2 promotion of TNF-α production by T cells (Extended Data Fig. 10l, m). In addition, when fetal T cells were cultured in the absence of cDC, they produced TNF-α, but when co-cultured with fetal cDC their ability to produce TNF-α was significantly impaired (Fig. 4g). Altogether, these data confirm that, in the absence of TLR stimulation, fetal dendritic cells promote immune suppression and impair T-cell TNF-α production in response to allogeneic antigens through expression of arginase-2. Importantly, a recent study highlighted the crucial role of L-arginine as major modulator of adult T-cell biology[24].

In summary, our findings have uncovered a previously unknown mechanism of tolerance and immune suppression that is used during gestation by fetal cDC and works in concert with other mechanisms used by fetal natural killer cells[25] and T_{reg} cells[1]. Understanding the mechanisms through which TNF-α production is regulated within the fetus is important, as elevated levels of TNF-α are associated with a number of pregnancy and perinatal complications including recurrent spontaneous miscarriage, gestational diabetes, and necrotizing enterocolitis. Our data suggest that the regulation of L-arginine levels by fetal dendritic cells is important for controlling T-cell TNF-α levels

during gestation, placing fetal dendritic cells as key regulators of TNF-α production that should be investigated as potential therapeutic targets in such situations. In addition, our study demonstrates that fetal cDC are immunologically dynamic and can orchestrate immune responses as early as the second trimester. How TLR stimulation during intrauterine infections can override immune suppression induced by arginase-2-expressing fetal dendritic cells in an allogeneic context remains to be explored. Altogether, these findings highlight that key processes in human immune development and programming in fact begin early during gestation and may have lifelong implications for immune homeostasis[19].

Online Content Methods, along with any additional Extended Data display items and Source Data, are available in the online version of the paper; references unique to these sections appear only in the online paper.

Received 11 August 2016; accepted 27 April 2017.
Published online 14 June 2017.

1. Mold, J. E. *et al.* Maternal alloantigens promote the development of tolerogenic fetal regulatory T cells in utero. *Science* **322,** 1562–1565 (2008).
2. Claas, F. H., Gijbels, Y., van der Velden-de Munck, J. & van Rood, J. J. Induction of B cell unresponsiveness to noninherited maternal HLA antigens during fetal life. *Science* **241,** 1815–1817 (1988).
3. de Vries, J. I., Visser, G. H. & Prechtl, H. F. The emergence of fetal behaviour. II. Quantitative aspects. *Early Hum. Dev.* **12,** 99–120 (1985).
4. Underwood, M. A., Gilbert, W. M. & Sherman, M. P. Amniotic fluid: not just fetal urine anymore. *J. Perinatol.* **25,** 341–348 (2005).
5. Campbell, D. E., Boyle, R. J., Thornton, C. A. & Prescott, S. L. Mechanisms of allergic disease—environmental and genetic determinants for the development of allergy. *Clin. Exp. Allergy* **45,** 844–858 (2015).
6. Aagaard, K. *et al.* The placenta harbors a unique microbiome. *Sci. Transl. Med.* **6,** 237ra65 (2014).
7. Haniffa, M. *et al.* Human tissues contain CD141^{hi} cross-presenting dendritic cells with functional homology to mouse CD103^{+} nonlymphoid dendritic cells. *Immunity* **37,** 60–73 (2012).
8. McGovern, N. *et al.* Human dermal CD14^{+} cells are a transient population of monocyte-derived macrophages. *Immunity* **41,** 465–477 (2014).
9. Schuster, C. *et al.* HLA-DR^{+} leukocytes acquire CD1 antigens in embryonic and fetal human skin and contain functional antigen-presenting cells. *J. Exp. Med.* **206,** 169–181 (2009).
10. Schlitzer, A., McGovern, N. & Ginhoux, F. Dendritic cells and monocyte-derived cells: two complementary and integrated functional systems. *Semin. Cell Dev. Biol.* **41,** 9–22 (2015).
11. Cheng, Y., Wong, M. T., van der Maaten, L. & Newell, E. W. Categorical analysis of human T cell heterogeneity with one-dimensional soli-expression by nonlinear stochastic embedding. *J. Immunol.* **196,** 924–932 (2016).
12. Guilliams, M. *et al.* Unsupervised high-dimensional analysis aligns dendritic cells across tissues and species. *Immunity* **45,** 669–684 (2016).
13. Ohl, L. *et al.* CCR7 governs skin dendritic cell migration under inflammatory and steady-state conditions. *Immunity* **21,** 279–288 (2004).
14. Förster, R., Davalos-Misslitz, A. C. & Rot, A. CCR7 and its ligands: balancing immunity and tolerance. *Nat. Rev. Immunol.* **8,** 362–371 (2008).
15. Wang, X.-N. *et al.* A three-dimensional atlas of human dermal leukocytes, lymphatics, and blood vessels. *J. Investig. Dermatol.* **134,** 965–974 (2013).
16. Haynes, B. F. & Heinly, C. S. Early human T cell development: analysis of the human thymus at the time of initial entry of hematopoietic stem cells into the fetal thymic microenvironment. *J. Exp. Med.* **181,** 1445–1458 (1995).
17. Schuster, C. *et al.* Development of blood and lymphatic endothelial cells in embryonic and fetal human skin. *Am. J. Pathol.* **185,** 2563–2574 (2015).
18. Tong, X. Amniotic fluid may act as a transporting pathway for signaling molecules and stem cells during the embryonic development of amniotes. *J. Chin. Med. Assoc.* **76,** 606–610 (2013).
19. Burlingham, W. J. *et al.* The effect of tolerance to noninherited maternal HLA antigens on the survival of renal transplants from sibling donors. *N. Engl. J. Med.* **339,** 1657–1664 (1998).
20. Liu, W. *et al.* CD127 expression inversely correlates with FoxP3 and suppressive function of human CD4^{+} T reg cells. *J. Exp. Med.* **203,** 1701–1711 (2006).
21. Seddiki, N. *et al.* Expression of interleukin (IL)-2 and IL-7 receptors discriminates between human regulatory and activated T cells. *J. Exp. Med.* **203,** 1693–1700 (2006).
22. Elahi, S. *et al.* Immunosuppressive CD71^{+} erythroid cells compromise neonatal host defence against infection. *Nature* **504,** 158–162 (2013).
23. Morris, S. M. Jr. Arginine: master and commander in innate immune responses. *Sci. Signal.* **3,** pe27 (2010)
24. Geiger, R. *et al.* L-arginine modulates T cell metabolism and enhances survival and anti-tumor activity. *Cell* **167,** 829–842 (2016).
25. Ivarsson, M. A. *et al.* Differentiation and functional regulation of human fetal NK cells. *J. Clin. Invest.* **123,** 3889–3901 (2013).

Supplementary Information is available in the online version of the paper.

Acknowledgements This work was supported by Singapore Immunology Network core funding (F.G. and E.W.N.), Biomedical Research Council (BMRC) Young Investigator Grant (N.McG.), Austrian Science Fund (P19474-B13, W1248-B30 to A.E.-B.), BMRC SPF2014/00 (S.A.), and the Singapore Ministry of Health's National Medical Research Council (J.K.Y.C, CSIRG/1383/2014, CSA(SI)/008/2016/). We thank L. Robinson for manuscript editing.

Author Contributions Conceptualization, N.McG., F.G., J.K.Y.C.; methodology, N.McG., F.G., A.S., G.L., D.L., L.J.T., R.M., I.L., N.B.S., H.R.S., E.S., J.L., E.M., S.H., P.S., B.J., C.S., A.E.-B., X.N.W., E.W.N.; clinicians for help accessing samples and for discussion, E.H.K., Y.H.L., M.C., C.N.Z.M., Y.F., T.K.H.L., D.K.H., K.-K.T., J.K.C.T., V.B., M.C., M.H., A.S., S.A., A.L., E.W.N.; bioinformatic analysis, N.McG., K.D., M.P., F.G.; writing, N.McG., F.G., J.K.Y.C.

Author Information Reprints and permissions information is available at www.nature.com/reprints. The authors declare no competing financial interests. Readers are welcome to comment on the online version of the paper. Publisher's note: Springer Nature remains neutral with regard to jurisdictional claims in published maps and institutional affiliations. Correspondence and requests for materials should be addressed to F.G. (Florent_Ginhoux@immunol.a-star.edu.sg) or J.K.Y.C. (jerrychan@duke.nus.edu.sg).

Reviewer Information *Nature* thanks V. Soumelis, S. S. Way and the other anonymous reviewer(s) for their contribution to the peer review of this work.

METHODS

Human samples and consent. The donation of fetal tissue for research was approved by the Centralised Institutional Research Board of the Singapore Health Services in Singapore. This approval strictly followed established international guidelines about the use of fetal tissue for research[26]. This approval allowed the collection of different fetal tissues from women undergoing clinically indicated termination of pregnancies for the study of immune cells. Women gave written informed consent for the donation of fetal tissue to research nurses who were not directly involved in the research, or in the clinical treatments of women participating in the study, as per the Polkinghorne guidelines[26]. This protocol was reviewed on an annual basis by the Centralised Institutional Research Board, including annual monitoring of any adverse events, for which there had been none. All fetal organs for this study (lung, thymus, spleen, MLNs, gut, appendix, liver, tonsil, and skin) were obtained during the second trimester (12–22 weeks EGA). All fetuses were considered structurally normal on ultrasound examination before termination and by gross morphological examination after termination. In total 72 fetuses of 12–16 weeks EGA and 24 fetuses of 17–22 weeks EGA were used for this study. For comparisons across fetal organs the same donors were used, for example for CyTOF data analysis.

Adult tissues (lung, spleen, gut, and skin) were obtained with approval from Singapore Singhealth and National Health Care Group Research Ethics Committees.

Cell isolation. Fetal organs were mechanically dispersed and incubated with 0.2 mg ml^{-1} collagenase (type IV; Sigma-Aldrich) and DNase I (20,000 U ml^{-1}; Roche) in Roswell Park Memorial Institute medium (RPMI) with 10% FCS for up to 1 h in a six-well plate. Viability was typically 80–90% measured by DAPI exclusion (Partec). Fetal gut was initially cut longitudinally through the centre, washed extensively in PBS until all inner content (meconium) was removed and the PBS was clear, before mechanical dispersion and digestion as above, for up to 1 h. Adult lung specimens (eight samples from different donors) were obtained from peri-tumoural tissue. Adult skin (20 samples from different donors) was obtained from mammoplasty and breast reconstruction surgery. Adult spleen specimens (eight samples from different donors) were obtained at distal pancreatectomies in patients with pancreatic tumours in the pancreas. Adult lung[27] and skin[8] specimens were prepared as described previously. Adult spleen specimens were prepared in a similar manner to lung. Tissue macrophages and dendritic cells were isolated to 95% purity from freshly digested tissue cell suspensions by fluorescence-activated cell sorting (FACS) using BD FACSAriaII or III (BD Biosciences). T cells were isolated to 90% purity from adult and fetal spleen by negative selection using T-cell enrichment kits (Miltenyi Biotec) and separated on an AutoMacs by following the manufacturer's instructions. T cells were labelled with 0.2 μM CFSE (Life Technologies) for 5 min at 37 °C. In all experiments, enriched APC and T cells were from fetal and adult spleen unless stated otherwise.

Flow cytometry. Flow cytometry was performed on a BDLSRII and data analysed with FlowJo (Treestar). Antibodies used are listed in Supplementary Table 12. An eBioscience FOXP3/Transcription Factor Staining Buffer Set (eBioscience/Affimetrix) was used for intracellular staining of IRF-8, IRF-4, CTLA4, arginase-2, TNF-α, and FOXP3 cells by following the manufacturer's instructions.

Mixed lymphocyte reactions. Five thousand sorted cDC from defined subpopulations were co-cultured with 100,000 CFSE-labelled adult or fetal spleen T cells for 6 days in 200 μl complete RPMI-1640 Glutamax medium (Life Technologies) supplemented with 10% FBS and 1% penicillin/streptomycin[27]. On day 6, cells supernatants (100 μl) were removed and stored at −80 °C for detection of the cytokines indicated in Fig. 4a and Extended Data Figs 8f and 10i–k) at a later date. Cytokines were detected using Luminex bead-based multiplex assays, as detailed below. For analysis of intracellular TNF-α production analysis, on day 6 of co-cultures T cells were re-stimulated with 10 μg ml^{-1} phorbol myristate acetate (PMA) and 500 μg ml^{-1} ionomycin for 1 h at 37 °C. Brefeldin A solution (10 μg ml^{-1}) was added for 4 h. Intracellular cytokine production was determined by flow cytometry. In some experiments on day 0, the arginase inhibitors *S*-(2-boronoethyl)-L-cysteine (BEC) or amino-2-borono-6-hexanoic acid (ABH) (each used at 30 μM respectively) were added to co-cultures. In some experiments on day 6, 1 mM L-arginine was added to co-cultures 1 h before stimulation with PMA/ionomycin.

***Ex vivo* co-culture assays.** Fetal or adult splenocytes (1×10^5) were seeded into 96-well round-bottom plates alone or combined at defined ratios in 200 μl medium. After co-culture overnight or for 6 days, the splenocytes were stimulated with 10 μg ml^{-1} PMA (InvivoGen) and 500 μg ml^{-1} ionomycin (Sigma) for 1 h at 37 °C. Brefeldin A solution (10 μg ml^{-1}) was added for 4 h. Intracellular T-cell TNF-α production was determined by flow cytometry as described above.

Millipore Luminex bead-based multiplex assays on supernatants from mixed lymphocyte reactions. Samples (supernatants) or standards were incubated with fluorescent-coded magnetic beads pre-coated with cytokine-specific capture antibodies. After an overnight incubation at 4 °C with shaking, plates were washed twice with wash buffer. Biotinylated detection antibodies specific to the cytokine of interest were incubated with the complex for 1 h and subsequently Streptavidin-PE was added and the complex incubated for another 30 min. Plates were washed twice again, and beads were re-suspended with sheath fluid before a minimum of 50 beads per cytokine were analysed on a Luminex FLEXMAP 3D (Merck Millipore). Data acquisition used xPONENT 4.0 (Luminex) acquisition software, with data analysed in Bio-Plex Manager 6.1.1 (Bio-Rad). Cytokine concentrations were calculated from the standard curve using a 5PL (5-parameter logistic) curve fit.

Drop array Luminex assays on fetal and adult spleen cDC2. Sorted fetal (17–22 weeks EGA) and adult spleen cDC2 were incubated for 18 h at 20,000 cells per well in 100 μl complete RPMI-1640 Glutamax medium (Life Technologies) supplemented with 10% FBS and 1% penicillin/streptomycin, and stimulated either with TLR agonists (CL075 (1 μg ml^{-1}), CpG (3 μM), PI:C (25 μg ml^{-1}), PGN (10 μg ml^{-1}), LPS (0.1 μg ml^{-1}) + CD40L (1 μg ml^{-1})) or with DMSO control. Cells were then pelleted and 95 μl of supernatants were collected. Fetal and adult spleen cDC2 cytokine production was assessed using Luminex bead-based multiplex assays. Cytokines indicated in the figures were detected with DropArray-bead plates (Curiox) according to the manufacturer's recommendations. Acquisition was performed with xPONENT 4.0 (Luminex) acquisition software, and data analysis with Bio-Plex Manager 6.1.1 (Bio-Rad).

Mass cytometry staining, barcoding, acquisition, and data pre-processing. For mass cytometry analysis, purified antibodies were obtained from Invitrogen, Fluidigm, Biolegend, eBioscience, Beckton Dickinson, and R&D Systems using clones as listed in Supplementary Table 13. For some markers, fluorophore- or biotin-conjugated antibodies were used as primary antibodies, followed by secondary labelling with anti-fluorophore metal-conjugated antibodies (that is, anti-FITC clone FIT-22) or metal-conjugated streptavidin produced as previously described[11]. Briefly, cells were plated, stained, and labelled in a V-bottom 96-well plate (BD Falcon). Cells were washed once with 200 μl FACS buffer (4% FBS, 2 mM EDTA, 0.05% Azide in 1× PBS), followed by staining with 100 μl of 200 μM cisplatin (Sigma-Aldrich) for 5 min on ice to exclude dead cells. Cells were then labelled with anti-CADM1-biotin and antibodies in a 50 μl reaction volume for 30 min on ice. Cells were washed twice with FACS buffer and labelled with 50 μl heavy-metal isotope-conjugated secondary antibody cocktail for 30 min on ice. Cells were washed twice with FACS buffer then once with PBS before fixation with 200 μl 2% PFA (Electron Microscopy Sciences) in PBS overnight or longer. After fixation, cells were pelleted and re-suspended in 200 μl 1× perm buffer (Biolegend) and allowed to stand for 5 min at room temperature. Cells were washed once with PBS before barcoding. Bromoacetamidobenzyl-EDTA (BABE)-linked metal barcodes were prepared by dissolving BABE (Dojindo) in 100 mM HEPES buffer (Gibco) to a final concentration of 2 mM. Isotopically purified $PdCl_2$ (Trace Sciences) was then added to BABE solution to 0.5 mM. Similarly, DOTA-maleimide-linked metal barcodes were prepared by dissolving DOTA-maleimide (Macrocyclics) in L buffer (MAXPAR) to a final concentration of 1 mM. Then, 50 mM of $RhCl_3$ (Sigma) and isotopically purified $LnCl_3$ were added to DOTA-maleimide solution to 0.5 mM. Six metal barcodes were used: BABE–Pd-102, BABE–Pd-104, BABE–Pd-106, BABE–Pd-108, BABE–Pd-110, and DOTA-maleimide–Ln-113. All BABE and DOTA-maleimide–metal solution mixtures were immediately snap-frozen in liquid nitrogen and stored at −80 °C. A unique dual combination of barcodes was chosen to stain each tissue sample. Barcode Pd-102 was used at 1:4,000 dilution, Pd-104 at 1:2,000, Pd-106 and Pd-108 at 1:1,000, and Pd-110 and Ln-113 at 1:500. Cells were incubated with 100 μl of barcodes in PBS for 30 min on ice. They were then washed in perm buffer and incubated in FACS buffer for 10 min on ice. Cells were then pelleted and re-suspended in 100 μl of nucleic acid Ir-Intercalator (MAXPAR) in 2% PFA/PBS (1:2,000), at room temperature. After 20 min, cells were washed twice with FACS buffer and twice with water before a final resuspension in water. In each set, cells were pooled from all tissue types, enumerated, and diluted to a final concentration of 0.5×10^6 cells per millilitre for acquisition. EQ Four Element Calibration Beads (DVS Science, Fluidigm) were added at a concentration of 1% before acquisition. Cells were acquired and analysed using a CyTOF Mass cytometer. The data were exported in traditional flow-cytometry-file (.fcs) format and cells for each barcode were deconvolved using Boolean gating.

One-SENSE analysis. The automated analysis used the One-SENSE algorithm as described previously[11]. For Fig. 2 and Extended Data Figs 4b and 5b, the lineage dimension included CD1c and SIRPα as cDC2 markers, and CD26 and CLEC9A as cDC1 markers. The marker dimension included all the other non-lineage markers of the CyTOF panel. Frequency heatmaps of indicated markers are displayed for both dimensions. cDC2 clusters (cyan gate) and cDC1 clusters (green gate) for each organ and their marker expression profile are highlighted by the extended gates (representative plots of $n = 5$). For comparisons across fetal organs, organs from the same donor were used.

Microarray analysis. Total RNA was isolated from FACS-purified fetal spleen and skin (17–22 weeks EGA) $CD14^+$, cDC1, and cDC2 cell subsets, and adult spleen $CD14^+$, cDC1, and cDC2 cell subsets, with a Qiagen RNeasy Micro kit (Qiagen). Total RNA integrity was assessed using Agilent Bioanalyzer and the RNA integrity number was calculated; all RNA samples had an RNA integrity number $\geq$7.1. Biotinylated complementary RNA was prepared according to the protocol by Epicentre TargetAmp 2-Round Biotin-aRNA Amplification Kit 3.0 using 500 pg of total RNA. Hybridization of complementary RNA was performed on Illumina Human-HT12 Version 4 chips. Microarray data were exported from GenomeStudio software without background subtraction. Expression values were quantile normalized and $\log_2$-transformed in R (version 3.1.2) with Bioconductor (version 2.26.0) lumi package (version 2.18.0). To generate fetal APC subset gene signatures, one cell subset was compared with other cell subsets pooled using *t*-test in R. Differentially expressed genes were selected with a Benjamini–Hochberg multiple testing[28] corrected *P* value of <0.05. For the adult APC gene expression data, samples were grouped by tissue type, and tissue-specific probes were identified with one-way analysis of variance (ANOVA) and a Benjamini–Hochberg multiple testing corrected *P* value of <0.05. Connectivity map analysis as previously described[11] was performed comparing fetal dendritic cell signature gene subsets with the adult APC gene expression data after removal of the tissue-specific probes (see Extended Data Fig. 3 for hierarchical clustering and PCA plots before and after removal of tissue-specific probes). To identify the genes that were highly or lowly expressed in a particular cell subset, we used the single-class rank product method[29], implemented in the Bioconductor RankProd package (version 2.38.0), and selected the top- and bottom-ranked genes with a percentage of false-positives less than 0.01. The in-house-generated adult and fetal microarray data have been deposited in the Gene Expression Omnibus under accession numbers GSE35457, GSE85305, and GSE85304.

Quantitative PCR. Total RNA was isolated from adult or fetal gut and MLN (14–20 weeks EGA) cells with a Qiagen RNeasy Micro kit (Qiagen). Total RNA integrity and concentration was assessed using nanodrop 2000 (Thermoscientific). Total RNA (1 μg) was reverse transcribed using oligo (dT)18 primer and SuperScript II reverse transcriptase (GIBCO-BRL). CCL19 and CCL21 expression was analysed by quantitative PCR using the following primers: +5-CCAGCCTCACATCACTCA CACCTTGC-3 and −5-TGTGGTGAACACTACAGCAGGCACCC-3 for CCL19; +5-AACCAAGCTTAGGCTGCTCCATCCCA-3 and −5-TATGGCCCTTTAGG GGTCTGTGACCG-3 for CCL21. CCL19 and CCL21 expression was normalized to the housekeeping gene GAPDH +5-GCCAAGGTCATCCATGACAACTTTGG-3 and −5-GCCTGCTTCACCACCTTCTTGATGTC-3.

Confocal microscopy. Samples were prepared for confocal microscopy as described previously[15].

Statistical analysis. Statistical analysis used for each experiment is indicated in the figure legends. Each *n* number represents an individual donor and a separate experiment, apart from CyTOF experiments as indicated in the Extended Data figure legends. No statistical methods were used to predetermine sample size. The experiments were not randomized. The investigators were not blinded to allocation during experiments and outcome assessment.

Data availability. Source data for number(s) are provided with the paper. Sequence data that support the findings of this study have been deposited in the Gene Expression Omnibus under accession numbers GSE35457, GSE85305, and GSE85304. Further data that support the findings of this study are available from the corresponding authors upon reasonable request.

26. Polkinghorne, J. *Review of the Guidance on the Research Use of Fetuses and Fetal Material* (Her Majesty's Stationery Office, 1989).
27. Schlitzer, A. *et al.* IRF4 transcription factor-dependent CD11b+ dendritic cells in human and mouse control mucosal IL-17 cytokine responses. *Immunity* **38,** 970–983 (2013).
28. Benjamini, Y., Drai, D., Elmer, G., Kafkafi, N. & Golani, I. Controlling the false discovery rate in behavior genetics research. *Behav. Brain Res.* **125,** 279–284 (2001).
29. Breitling, R., Armengaud, P., Amtmann, A. & Herzyk, P. Rank products: a simple, yet powerful, new method to detect differentially regulated genes in replicated microarray experiments. *FEBS Lett.* **573,** 83–92 (2004).

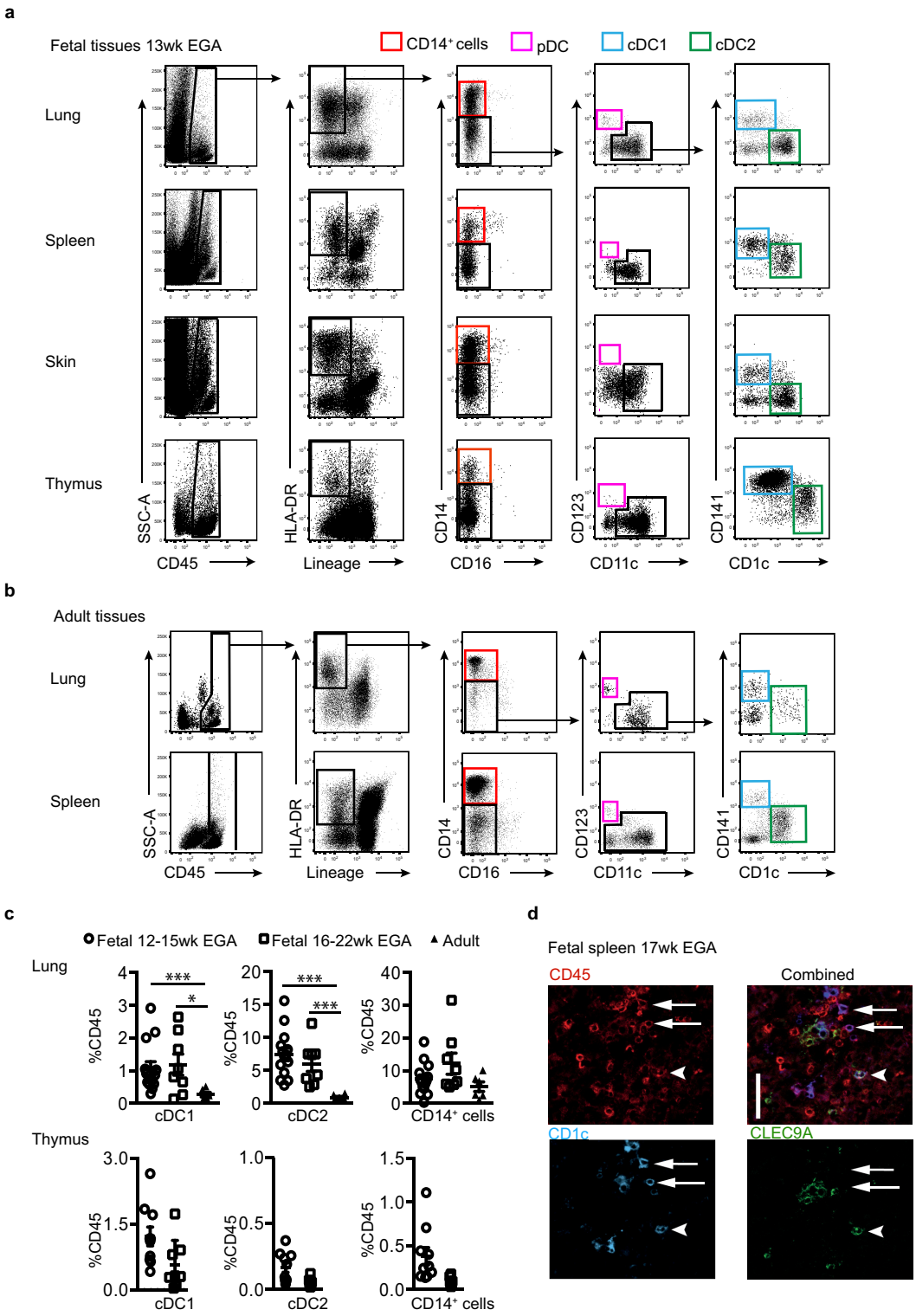

Extended Data Figure 1 | Identification of APC subsets in fetal and adult tissues. Representative flow plots of gating strategy used to identity APC subsets in fetal and adult tissues. **a**, Gating strategy used to identify APC populations within the live CD45$^+$, HLA-DR$^+$Lin$^-$ gate; CD14$^+$ (red gate), pDC (pink gate), cDC1 (blue gate), and cDC2 (green gate) cells in fetal lung, spleen, skin, and thymus. **b**, Gating strategy used to identify CD14$^+$ (red gate), pDC (pink gate), cDC1 (blue gate), and cDC2 (green gate) cells in adult lung and spleen. **c**, Abundance of APC plotted as a percentage of live CD45$^+$ mononuclear cells. Cell abundance was determined in fetal lung and thymus at two time points within the second trimester (12–15 weeks EGA) (circle, lung $n = 13$, thymus $= 9$) and 16–22 weeks EGA (square, lung $n = 8$, thymus $n = 8$) and compared with adult tissues (triangle, lung $n = 8$). Mean ± s.e.m. $^*P < 0.05$, $^{***}P < 0.001$, Mann–Whitney test. **d**, Pseudo-colour images of whole-mount fetal spleen (17 weeks EGA) immunolabelled for CD45 (red), CD1c (blue), and CLEC9A (green). White arrows highlight cDC2 (CD45$^+$CD1c$^+$CLEC9A$^-$), white arrowhead highlights cDC1 (CD45$^+$CD1c$^+$CLEC9A$^+$). Scale bar, 5 μm. Representative image of $n = 3$ experiments shown.

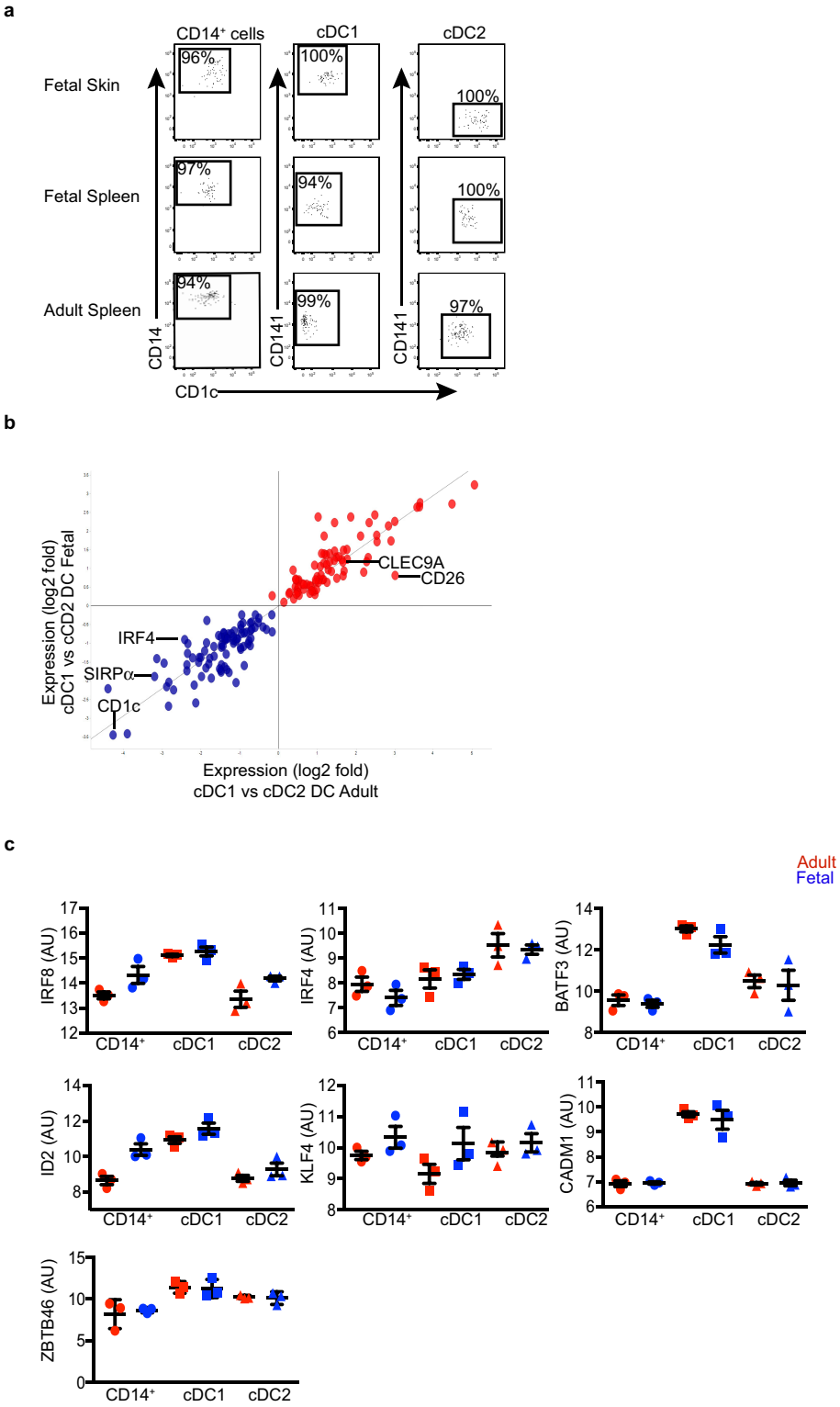

Extended Data Figure 2 | Comparison of the transcriptomes and phenotypes of fetal and adult APC subsets. a, Confirmation of post-sort APC subset purity. Representative dot plots demonstrating cell purity after using FACS to isolate indicated APC subsets from fetal skin and spleen (18–22 weeks EGA), and adult spleen; $n = 4$. **b**, Scatter plot of the log(fold change) in gene expression of cDC2 versus cDC1 from fetal and adult skin and spleen. $R = 0.92$ and $P < 2.2 \times 10^{-16}$. Colours indicate genes upregulated (red) or downregulated (blue) in fetal and adult cDC1 relative to cDC2. **c**, Scatterplots demonstrating the expression profile of transcription factors important for APC development[10], conserved across fetal (blue) and adult (red) spleen. Mean ± s.e.m.

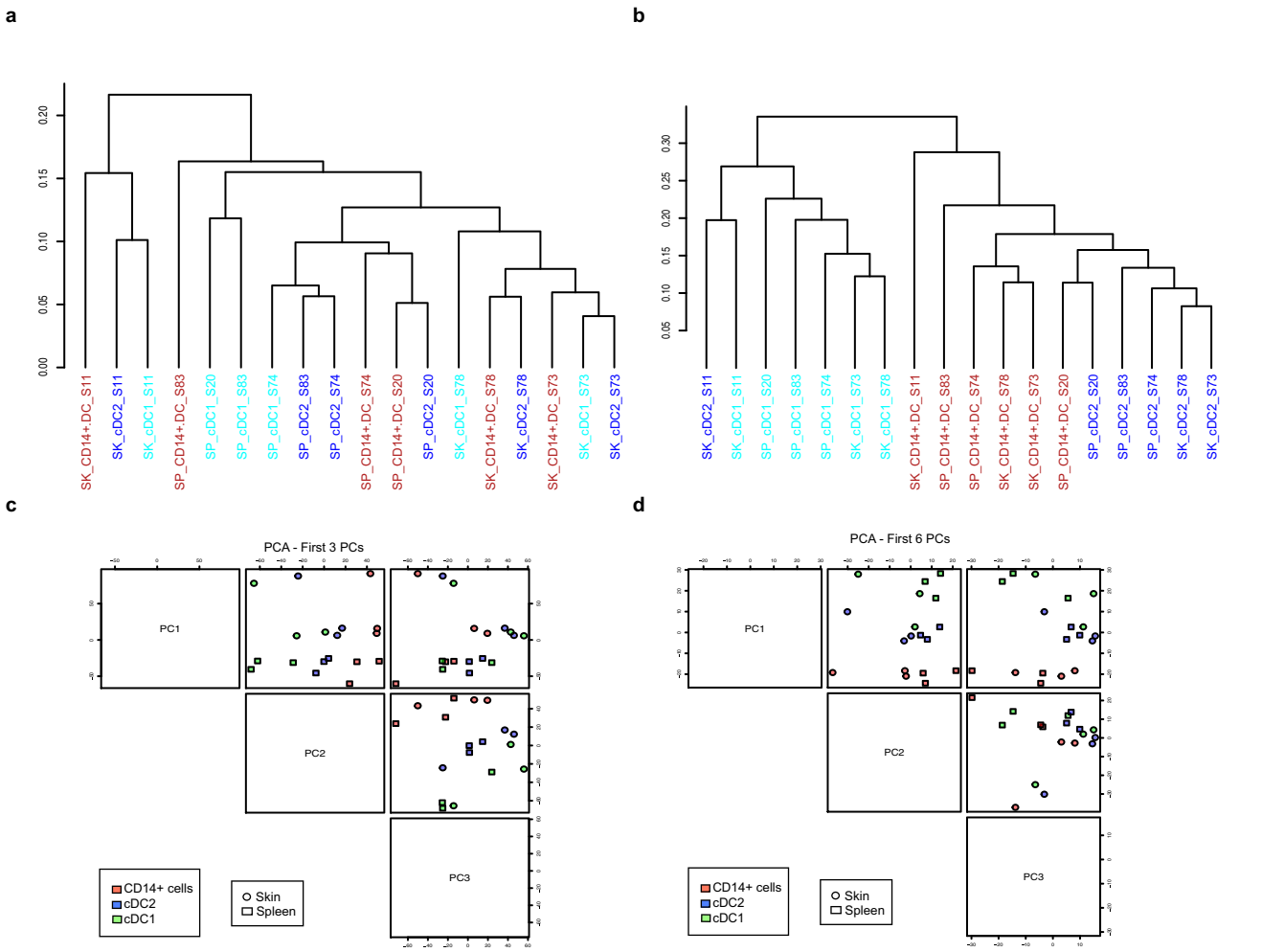

Extended Data Figure 3 | Fetal APC populations cluster based on subset after the removal of tissue-specific probes. a–d, Hierarchical clustering and PCA data before (**a**, **c**) and after (**b**, **d**) removal of tissue-specific probes. It is clear from the hierarchical clustering (**a**) that there is strong tissue imprinting in the cells that overwhelms subtype specificity. Upon the removal of tissue-specific probes, cells now cluster based on subtype (**b**). Also clearly from the PCA plots (**c**, **d**), we can see that before tissue gene removal (**c**), PC1 is entirely determined by tissue. However, upon tissue-specific probe removal (**d**), PC1 is now devoted to cell type. We identified these tissue-specific genes by finding differentially expressed genes between the pools of all cells from the different tissues (all spleen versus all skin).

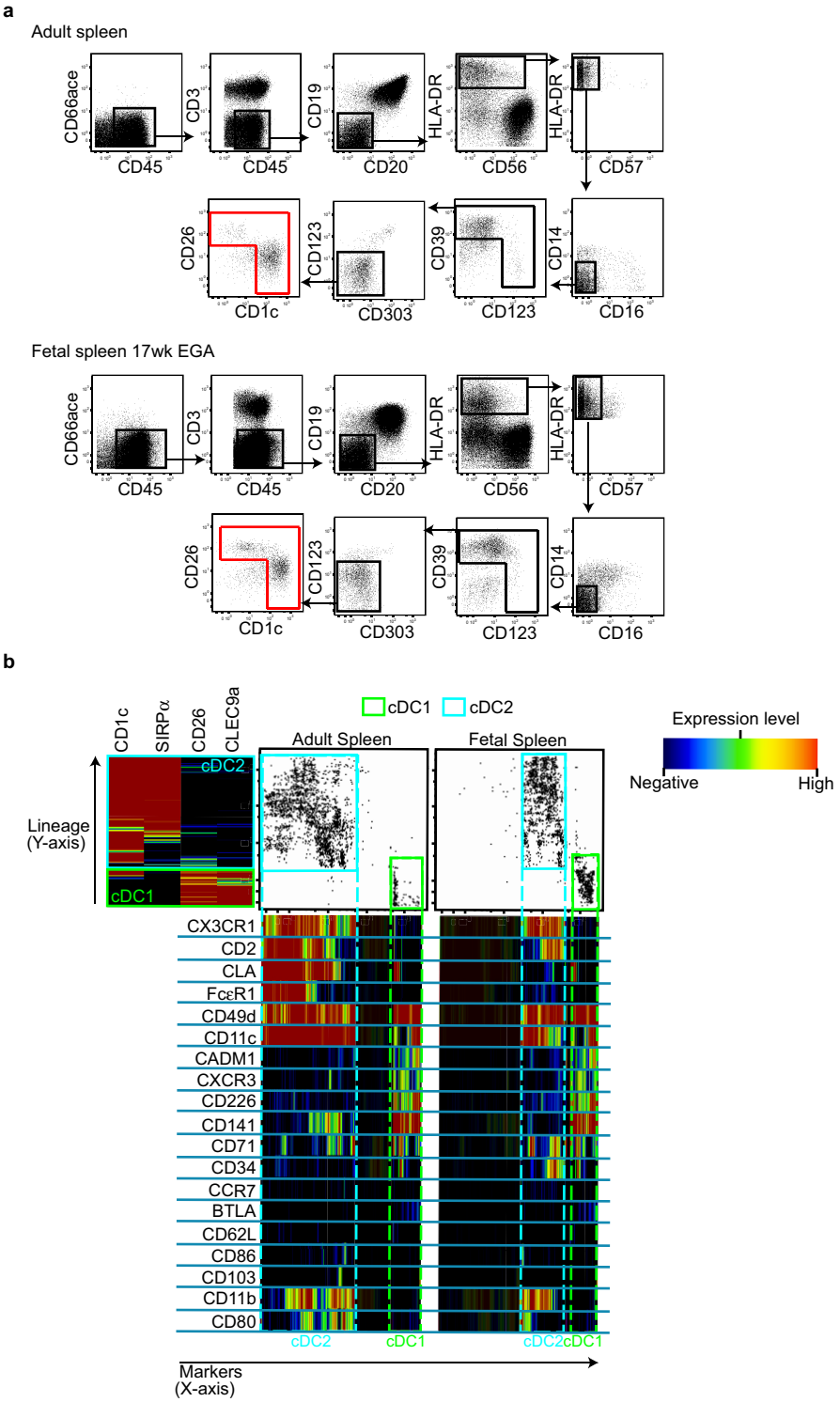

Extended Data Figure 4 | Fetal and adult spleen cDC have similar phenotypes. a, **b**, Characterization of cDC1 (green gate) and cDC2 (cyan gate) across adult and fetal spleen using CyTOF and One-SENSE algorithm[11]. **a**, Representative gating strategy used to select input population (red gate) for One-SENSE analysis from fetal (17 weeks EGA) and adult spleen samples. **b**, Representative data of fetal and adult spleen cDC analysed using the One-SENSE algorithm. The lineage dimension included CD1c and SIRPα as cDC2 markers, and CD26 and CLEC9A as cDC1 markers. The marker dimension included all the other non-lineage markers of the CyTOF panel. Frequency heatmaps of markers expression are displayed for both dimensions. The expression of markers by both adult and fetal spleen cDC1 (green) and cDC2 (cyan) is highlighted with the dashed gates. Representative data from $n = 5$ donors over two separate experiments.

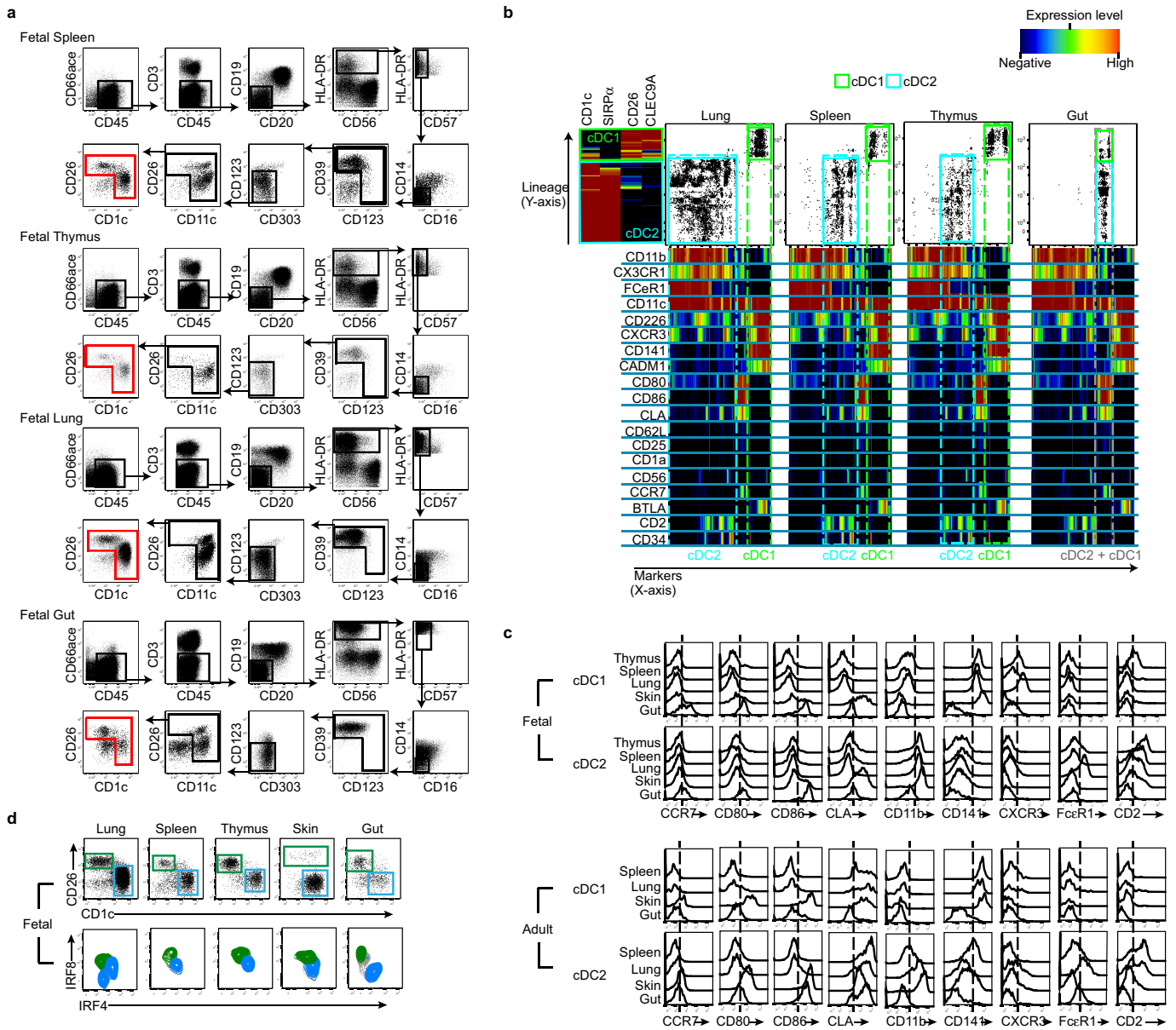

Extended Data Figure 5 | Phenotypic characterization of fetal spleen, thymus, lung, and gut cDC. a, Representative gating strategy used to select input population (red gate) for One-SENSE analysis from fetal spleen, thymus, lung, and gut (17 weeks EGA). **b**, Characterization of cDC1 (green gate) and cDC2 (cyan gate) across fetal lung, spleen, thymus, and gut using CyTOF and One-SENSE algorithm[11]. The lineage dimension included CD1c and SIRPα as cDC2 markers, and CD26 and CLEC9A as cDC1 markers. The marker dimension included all the other non-lineage markers of the CyTOF panel. Frequency heatmaps of markers expression are displayed for both dimensions. The expression of markers by fetal cDC1 (green) and cDC2 (cyan) subsets are highlighted with the dashed gates. Representative data from $n = 5$ donors over two separate experiments. **c**, Histograms displaying surface markers differentially expressed across fetal organs (17 weeks EGA) but conserved from fetus to adult. The histograms are generated from CyTOF data (generated as described above). Data are representative of $n = 5$ donors over two separate experiments. **d**, Fetal cDC1 (green gate) and cDC2 (blue gate) populations were identified within each organ on the basis of their CD26 and CD1c expression (top panels) by flow cytometry analysis. Using the gates in the top panels to select fetal cDC1 (green contours) and cDC2 (blue contours), intracellular expression of IRF-8 and IRF-4 was determined by flow cytometry. Representative data; $n = 3$ donors in three experiments.

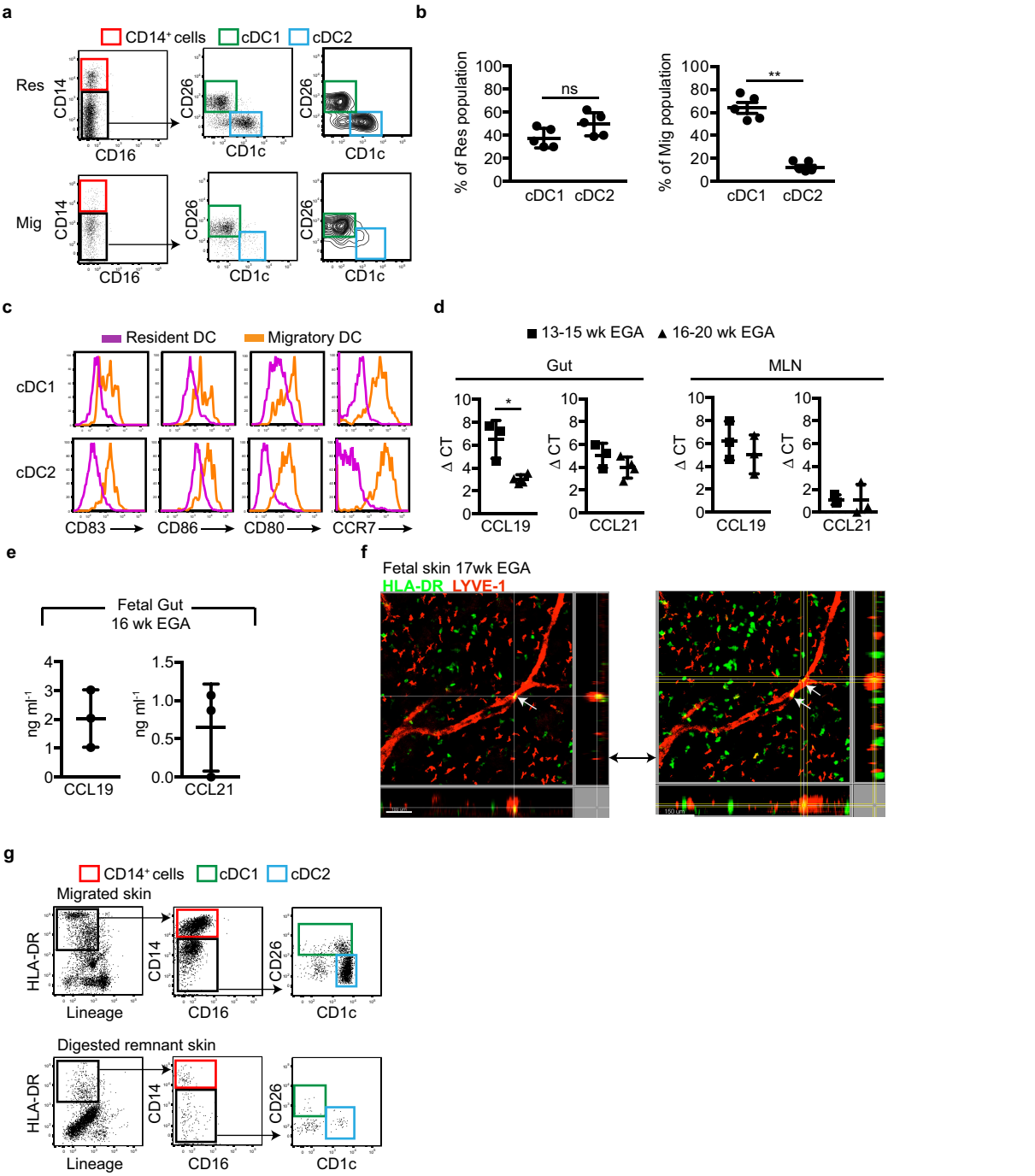

Extended Data Figure 6 | Fetal cDC migrate to lymph nodes. **a**, Representative plot of $CD14^+$ cells (red gate), cDC1 (green gate), and cDC2 (blue gate) identified within the MLN-resident (Res) dendritic cell gate (top panels) and migratory (Mig) dendritic cell gate (bottom panels), from a 16 week EGA sample. **b**, Abundance of cDC1 and cDC2 plotted as a percentage of the total cDC within the resident (left) and migratory (right) fraction within the MLN from 16 to 22 weeks EGA ($n = 5$). Mean ± s.e.m. **c**, Histograms comparing the expression of activation markers by resident (pink) and migratory (orange) cDC1 and cDC2 ($n = 3$). **d**, RNA from fetal gut and MLN were analysed for the expression of CCL19 and CCL21 from early (13–15 weeks EGA) and late (16–20 weeks EGA) samples ($n = 3$). Mean ± s.e.m. **e**, Detection of the proteins CCL19 and CCL21 from lysed fetal gut cells by enzyme-linked immunosorbent assay ($n = 3$). Mean ± s.e.m. **f**, Whole-mount immunofluorescence microscopy of 17 week EGA fetal skin from two plains of view. Lymphatic vessels are labelled for LYVE-1 (red), APC are labelled for HLA-DR (green). White arrow indicates APC within lymphatic vessels. Scale bar, 100 μm (left) and 150 μm (right). Representative image of $n = 3$ experiments shown. **g**, Gating strategy used to identify $CD14^+$ (red gate), cDC1 (green gate), and cDC2 (blue gate) cells within the supernatant from fetal skin explant left for 48 h in culture and the digested remnant. Representative plots of $n = 3$ experiments shown.

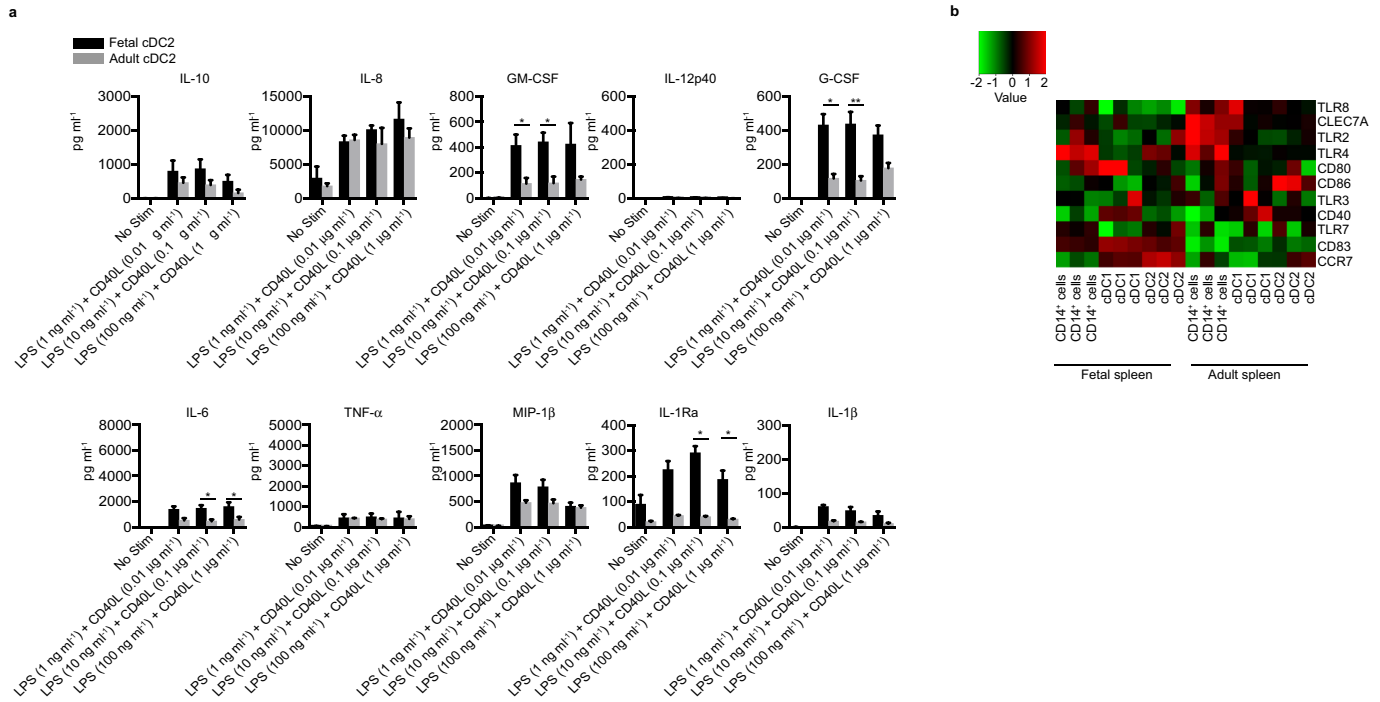

Extended Data Figure 7 | Fetal cDC are sensitive to low concentrations of TLR agonist stimuli. a, Sort-purified fetal liver and adult spleen cDC2 were cultured with the indicated TLR agonists for 18 h. Cytokines produced were measured in the supernatants by Luminex assay ($n = 3$). Mean ± s.e.m. **b**, Heatmap of fetal and adult spleen APC populations of selected genes, including pathogen recognition receptors and co-stimulatory molecules. Heatmap shows the row-based, *z*-score-normalized gene expression intensities.

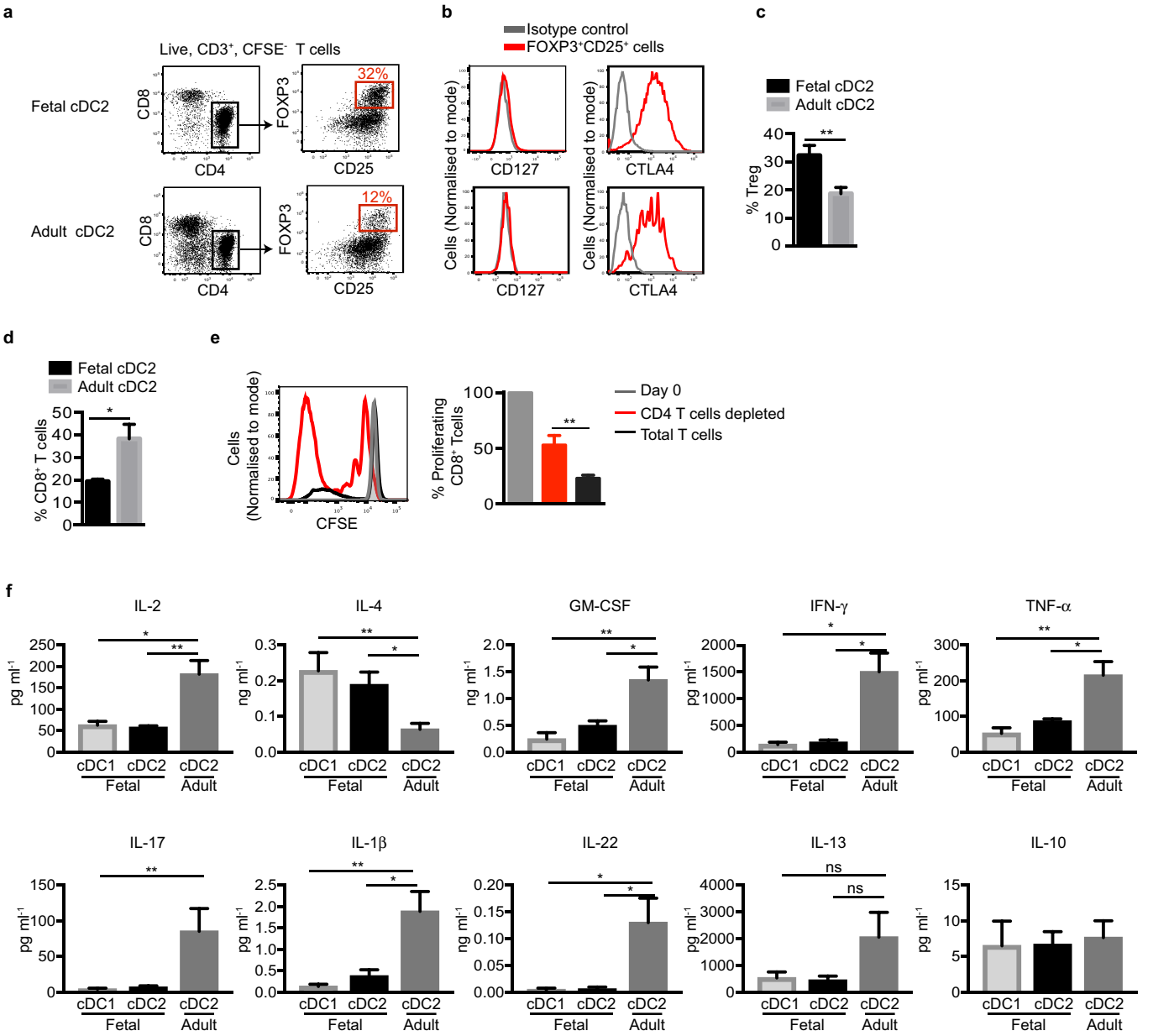

Extended Data Figure 8 | Fetal cDC promote T_{reg} induction. a–c, Flow cytometry expression analysis of T_{reg} cells after co-culture for 6 days of adult spleen T cells with fetal ($n = 5$) or adult ($n = 4$) spleen cDC2. **a**, **b**, Frequency of FOXP3$^+$CD25$^+$ T_{reg} cells (**a**, red gate) and representative histograms of the intensity of CD127 and CTLA-4 expression by T_{reg} cells (red histograms) and respective isotype controls (grey histograms) are shown (**b**). **c**, Composite results showing the frequency of T_{reg} cells plotted as percentage of CD4$^+$ T cells ($n \geq 4$). Mean ± s.e.m. **d**, Bar graph of proliferating CD8$^+$ T cells after 6 days of adult spleen pan T-cell co-culture with fetal (black, $n = 4$) or adult (grey, $n = 4$) spleen cDC2. Proliferation was measured by CFSE dilution. Mean ± s.e.m. **e**, Proliferation of isolated adult spleen CD8$^+$ T cells, after co-culture with fetal spleen cDC2 for 6 days. Left, representative histograms showing CFSE dilution by CD8$^+$ T cells on day 0 (grey histogram) compared with day 6 with (red histogram) or without (black histogram) CD4$^+$ T-cell depletion. Right, cumulative data ($n = 4$). Mean ± s.e.m. $*P < 0.05$, $**P < 0.01$, Mann–Whitney test. **f**, Fetal spleen cDC1 and cDC2 share immune-suppressive properties. Cytokine detected in co-culture supernatants after T-cell co-culture with fetal cDC1 or cDC2 or adult cDC2 ($n = 5$). Mean ± s.e.m. Statistical significance represents comparisons between indicated conditions measured by one-way ANOVA, multiple comparisons test. $*P < 0.05$; $**P < 0.01$; $***P < 0.001$; NS, $P > 0.05$.

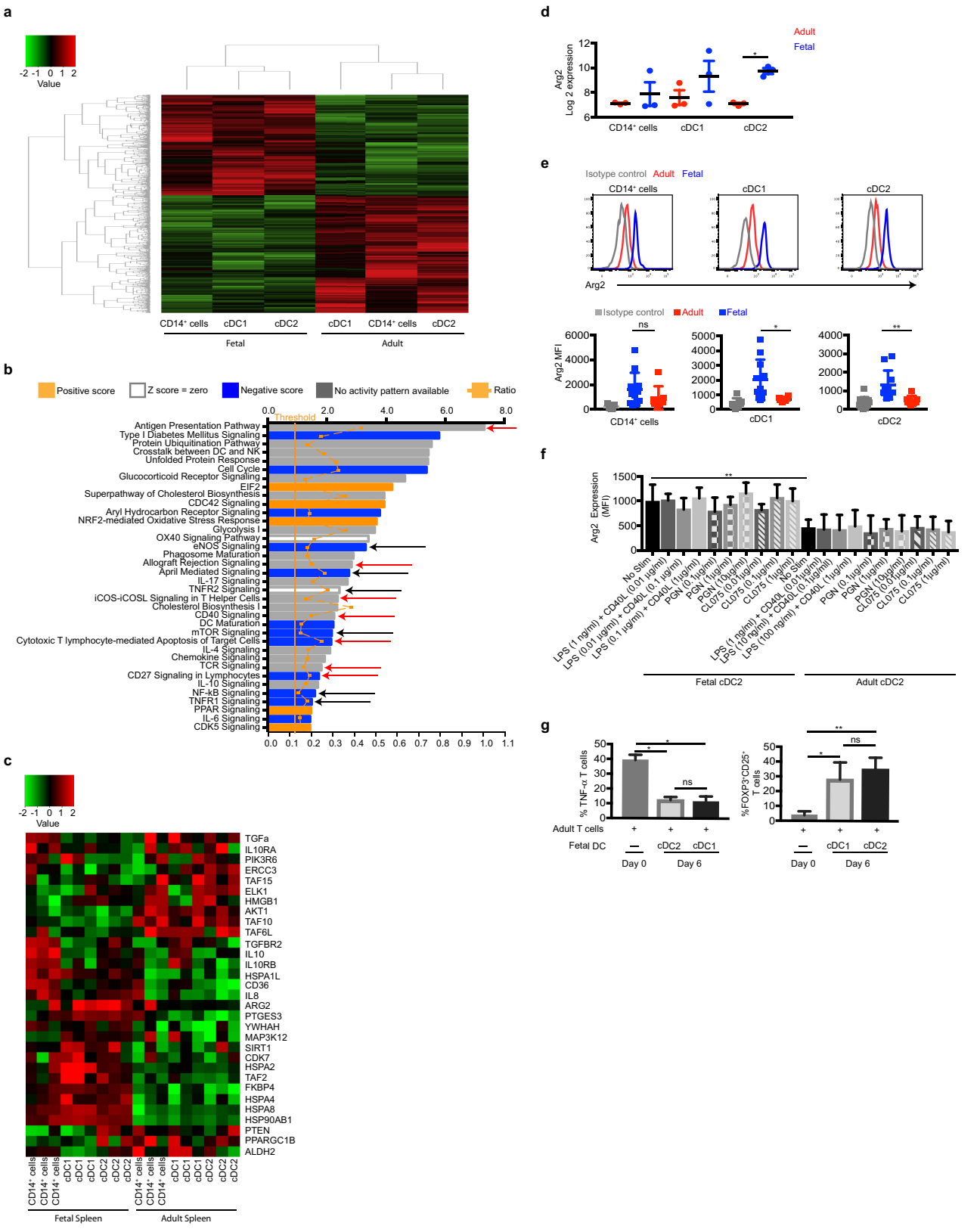

Extended Data Figure 9 | See next page for caption.

Extended Data Figure 9 | Gene expression comparison between fetal and adult APC. a, Heatmap showing the row-based, *z*-score-normalized gene expression intensities of 3,909 differentially expressed genes between fetal and adult APC. Differentially expressed genes were identified using a *t*-test with a Benjamini–Hochberg multiple testing corrected *P* value of <0.05. The genes and cell populations were clustered using the Pearson correlation distance measure and complete linkage method. **b**, Ingenuity pathway analysis of the differentially expressed genes, >1.5-fold change, between fetal and adult APC. Bars indicate the *P* values ($-\log_{10}$) for pathway enrichment. Orange squares indicate the ratio of the number of up- or downregulated genes mapped to the enriched pathway, to the total number of molecules on that pathway represented by the dashed orange line. The vertical solid orange line corresponds to the >1.5-fold change threshold. Red arrows highlight pathways involved in DC:T-cell interactions, black arrows highlight pathways associated with iNOS/TNF-α signalling. **c**, Heatmap of immune-modulatory genes involved in cellular metabolism, immune suppression, and the iNOS/TNF-α signalling. Heatmap shows the row-based, z-score-normalized gene expression intensities. **d**, **e**, Microarray (**d**) and flow cytometry (**e**) data demonstrating arginase-2 (Arg2) expression by fetal (blue, $n=11$) and adult (red, $n=7$) APC subsets. Isotype control, grey histogram and square on scatterplot ($n=7$). Mean ± s.e.m. **f**, Fetal and adult cDC2 arginase-2 expression is not mediated by TLR stimulation. Fetal liver and adult spleen cDC2 were sort-purified and stimulated with the indicated TLR agonists or dimethylsulfoxide (DMSO) control for 18 h. cDC2 arginase-2 expression was measured by flow cytometry. Mean ± s.e.m. One-way ANOVA, multiple comparisons test. $^{**}P<0.01$. **g**, TNF-α ($n=4$) and Treg ($n=4$ and 6) induction after adult spleen T-cell overnight culture alone or with fetal cDC1 or cDC2 for 6 days. Mean ± s.e.m.

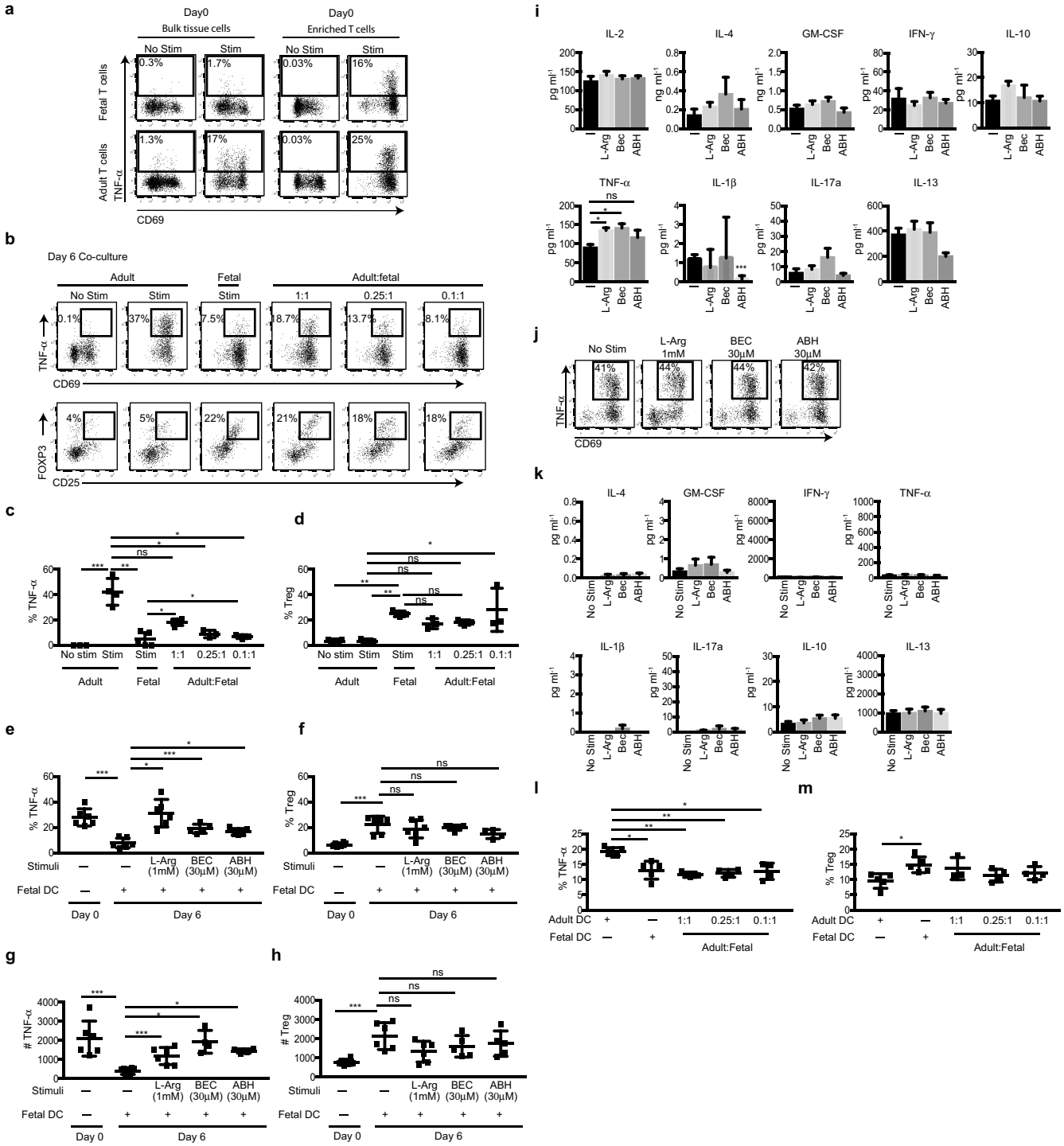

Extended Data Figure 10 | See next page for caption.

Extended Data Figure 10 | Fetal cDC regulate T-cell TNF-α production. **a**, *Ex vivo* splenocyte T-cell (bulk tissue cells) and enriched spleen T-cell TNF-α production, representative plots of $n = 4$. **b**, *Ex vivo* co-culture assay where fetal and adult splenocytes were cultured alone or at the indicated ratios of adult:fetal cells ($n = 3$–4) for 6 days. TNF-α^+ and T_{reg} cell induction was determined by flow cytometry analysis. **c**, **d**, Scatterplots demonstrating the percentage of TNF-α^+ T cells and T_{reg} after the culture of splenocytes under the indicated conditions for 6 days ($n \geq 3$). Mean ± s.e.m. Statistical significance represents comparisons between indicated conditions measured by one-way ANOVA, multiple comparisons test. *$P < 0.05$; **$P < 0.01$; ***$P < 0.001$; NS, $P > 0.05$. **e**–**h**, Scatterplots demonstrating the percentage (**e**, **f**) and absolute cell counts (**g**, **h**) of TNF-α^+ T cells and T_{reg} after overnight culture of adult spleen T cells alone ($n = 6$) or co-culture for 6 days with fetal cDC2 in the absence ($n = 6$) or presence ($n = 6$) of L-arginine, ABH ($n = 4$), or BEC ($n = 5$). Mean ± s.e.m. Statistical significance represents comparisons between indicated conditions measured by one-way ANOVA, multiple comparisons test. *$P < 0.05$; ***$P < 0.001$; NS, $P > 0.05$. **i**, Fetal dendritic cell arginase activity impacts T-cell TNF-α production but not other pro-inflammatory cytokines. Cytokines detected in co-culture supernatants after adult spleen T-cell co-culture with fetal cDC2 in the absence ($n = 5$) or presence of L-arginine (1 mM) ($n = 5$), BEC (30 μM) ($n = 3$), ABH (30 μM) ($n = 5$) for 6 days. Mean ± s.e.m. Statistical significance represents comparisons between indicated conditions measured by one-way ANOVA, multiple comparisons test. *$P < 0.05$; **$P < 0.01$; NS, $P > 0.05$. **j**, Adult spleen T cells were cultured overnight with the indicated of L-arginine, BEC, and ABH ($n = 5$). Representative flow cytometry plots. **k**, Cytokines detected in supernatants after adult spleen T cells were cultured alone (in the absence of dendritic cells) for 6 days with or without L-arginine (1 mM), BEC (30 μM), and ABH (30 μM) ($n = 5$). Mean ± s.e.m. **l**, **m**, Fetal spleen cDC (pooled cDC1 and cDC2) and adult spleen cDC2 were cultured alone or in combination at the indicated ratios with adult spleen T cells for 6 days. T-cell TNF-α production (**l**) and the expansion of T_{reg} cells (**m**) were assessed by flow cytometry. Statistical significance represents comparisons between indicated conditions measured by one-way ANOVA, multiple comparisons test. *$P < 0.05$; NS, $P > 0.05$. Each data point in all the scatter plots represents an individual donor and experiment. Mean ± s.e.m.